ISBN: 978-3-95450-214-1 ISSN: 2673-5490 doi:10.18429/JACoW-IPAC2021-WEPAB355

# SERIES PRODUCTION OF THE SIS100 CRYOCATCHERS

L .H. J. Bozyk*, S. Ahmed, P. J. Spiller
GSI Helmholtzzentrum für Schwerionenforschung, Darmstadt, Germany

*Abstract*

The superconducting heavy ion synchrotron SIS100, which is the main accelerator of the FAIR-facility, will be equipped with cryocatchers to suppress dynamic vacuum effects and to assure a reliable operation of high intensity heavy-ion beams. Subsequent to the successful validation of the prototype in 2011 and a First-of-Series cryocatcher in 2018, the series production of 60 cryocatcher modules meanwhile has been completed. It was released in 2018 after further design optimizations. Key findings from the series production and acceptance tests are presented as well. The First-of-Series cryocatcher has been integrated into the First-of-Series quadrupole module and has undergone several tests. These results are also illustrated in this report.

## INTRODUCTION

The ion optical layout of the FAIR synchrotron SIS100 has been optimized such, that stripped reference beam ions ($U^{28+}$) are lost at well defined and highly localized positions in the cryogenic arcs. In total 60 ion catchers will be installed at these positions, providing a perpendicular low desorption surface, to suppress dynamic vacuum effects. They are operated in a cryogenic environment, which gave the name 'cryocatcher'.

The chamber of the cryocatcher acts as a cryopump and provides a high pumping surface. Desorbed gases, which are relesed by ion impact are bound quickly onto these cryogenic walls. Such, further charge exchange of beam ions is minimized. A homogeneous low temperature distribution is achieved by a copper plating of the outer surface of the stainless steel vacuum chamber. A special support structure of the actual cryocatcher block allows keeping it at a higher temperature, than the chamber, in order to avoid gas particles to be bound at the ion impact area. This support will be connected to the thermal shield of the cryostat, whereby the heat, deposited by the lost beam ions, is lead away by the shield cooling at 50 K - 70 K, instead of the magnet cooling at 4.2 K.

A prototype cryocatcher has been developed [1], built, and tested [2–4]. For the series cryocatchers, several modifications had to be implemented and a First-of-Series (FoS) Cryocatcher has been manufacured [5]. After intensive testing of the mechanical, vacuum and cryogenic properties of the FoS-crocatcher, and a procedure test of the brazing process, the series production was launched after minor modifications in September 2018. Figure 1 shows several cryocatcher modules during site acceptance test at GSI.

* L.Bozyk@gsi.de

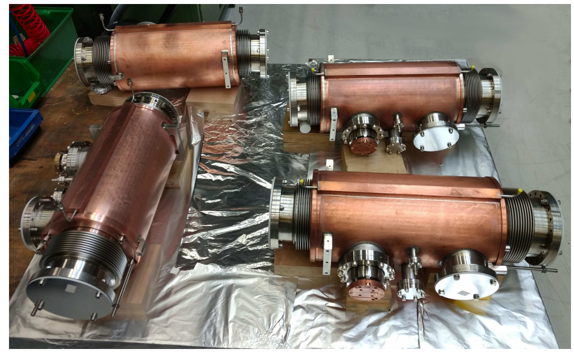

Figure 1: Series cryocatcher modules during site acceptance test at GSI.

## SERIES PRDUCTION OF SIS100 CRYOCATCHER

After the manufacturing process of a cryocatcher chamber, it underwent a set of tests at the manufacturer's place, called Factory Acceptance Test (FAT). The finished FAT marks the end of the manufacturing process and its release allows the delivery to GSI. Figure 2 shows the number of finished FATs per month during the series production. The last chambers were delivered in December 2020, resulting in a total production time of 28 months for 61 series cryocatchers.

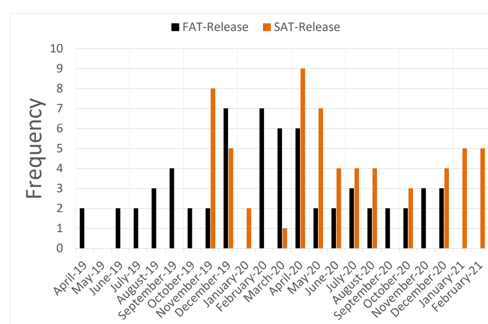


Figure 2: Number of finished Factory and Site Acceptance Tests (FAT and SAT) per month during series production.

Figure 2 also shows the rate of finished Site Acceptance Tests (SAT). The acceptance rate is slightly shifted with respect to the acceptance rate, since the first chambers needed rework by the manufacturer after delivery to GSI.

## ISSUES DURING THE SERIES PRODUCTION

The most common issues during the series production concerned the position of the threaded holes for the fixation

12th Int. Particle Acc. Conf. IPAC2021, Campinas, SP, Brazil JACoW Publishing
ISBN: 978-3-95450-214-1 ISSN: 2673-5490 doi:10.18429/JACoW-IPAC2021-WEPAB355



downstream. Despite several optimizations of the milling sequence, the specified position tolerance of 0.5 mm could not be reached for certain. Figure 3 shows the distribution of measured thread tolerances, the average is 0.35 mm. It has to be admitted, that measuring the position tolerance of a thread is a challenge for its own. All chambers with positions outside the tolerance were evaluated individually, checked with a template, and non-conformity-reports were written, when the risk for non-fitting in the integration was assumend small.

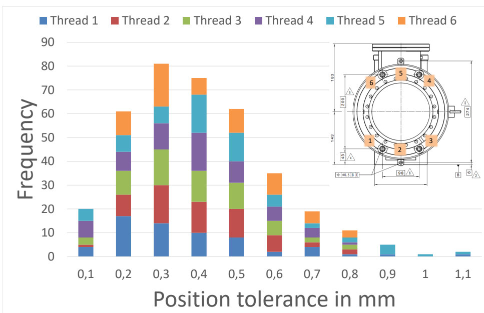


Figure 3: Achieved position tolerance of the six M10 thread holes for the fixation downstream. The specified tolerance is 0.5 mm.

Another common issue was the cooling pipe. The sticking out pipes from time to time were subject to deformation, but the brazing process itself also could not reach a sufficient reproducibility. The brazing seam between cooling profile and chamber had to be reworked for several chambers, therefore a manual reworking procedure including flame brazing was developped. The brazing seam between the cooling profile and the cooling pipes had to be reworked for several chambers as well. Here, reworking means cutting off the whole cooling profile and rebrazing a new one with manual flame brazing.

## FACTORY AND SITE ACCEPTANCE TESTS

Each FAT consists of several parts:

- During **visual inspection** the outer appearance is checked. Annealing colours and scratches as well as the quality of soldering seams are examinated.
- The **electrical tests** check for the internal electrical connection of the insulated front part of the cryocatcher block and the functionality of the temperature sensor.
- Measurements of defined mechanical tolerances are done during **mechanical tests**. In particular interfaces to superior components are measured, but also the position tolerance of the actual cryocatcher inside the chamber.
- The **vacuum tests** start with a leak test before a bake-out of the chamber for 7 days at 250°. Afterwards, the outgassing rate is determined, and a residual gas spectrum is analyzed to confirm the cleanliness of inner surfaces. The tests are finished with another leak test after bake-out.
- The **cooling pipe** is tested for its leak rate, residual moisture, flow rate and underwents a pressure test according to pressure vessel regulations AD2000.
- At the end a set of **certificates** for material and personal is added to the documentation.

The distribution of all measured collimator distances to the beam axis are shown in Fig. 4, it is specified to 40 mm ±0.5 mm. The angles to the beam axis shall be 3° ± 0.1°, the distribution of all measured angles is shown in Fig. 5. The measurments show, that all collimators tend to be further away and more tilted, than specified. That means no unexpected obstacles for the beam have to be expected.

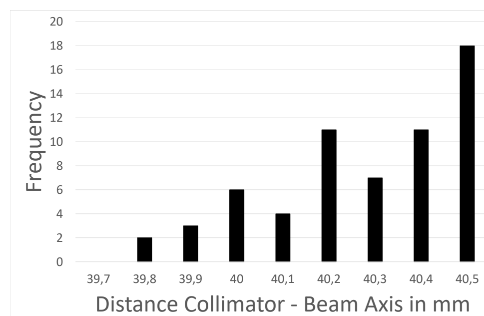


Figure 4: Frequency distribution of distances beween beam axis and collimator block. It is specified to 40 ± 0.5 mm.

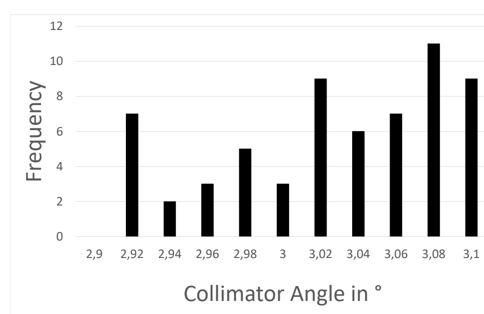


Figure 5: Frequency distribution of angles beween beam axis and collimator block. The specification is 3° ± 0.1°.

In average a final pressure of $1.49 \cdot 10^{-10}$ mbar was reached, which yields in an average outgassing rate of $5.44 \cdot 10^{-13}$ mbar l/(s cm$^2$). The specified maximum outgassing rate is $< 1 \cdot 10^{-12}$ mbar l/(s cm$^2$).

ISBN: 978-3-95450-214-1 ISSN: 2673-5490 doi:10.18429/JACoW-IPAC2021-WEPAB355

After the standardized release process of a FAT, the chambers were delivered to GSI, where another set of tests during the SAT heve been perfomed:

- In the **incomming goods inspection** the transport boxes are checked for damages and the content for completeness.
- During the **visual tests**, the labels of the component and indivudual parts were checked. The conditions of cutting edged of the conflat-flanges were inspected. All screw connections were checked and the brazed connection were inspected for imperfections.
- A set of **electrical tests** confirms the connection to the cryocatcher block and the functionality of the temperature sensor.
- The **interface test** checks if no obvious deformations are present, all threads and dowel pin holes are fine. In particular deformations at the helium pipes were discovered here.
- The **electrical capacity** between collimator block and its cabling and the surrounding chamber was measured and documented. This will be used to confirm the correct cabling inside the integrated quadrupole module.
- Finally a small **vacuum test** consisting of a leak test was performed.

After the SAT, a release procedure was launched and the accepted cryocatcher module was either delivered to the company integrating the quadrupole module, or stored on site.

## TESTS INSIDE THE FOS QUADRUPOLE MODULE

Meanwhile the FoS cryocatcher has been integrated into the FoS quadrupole module and underwent a new set of tests. The correct cabling to the cryocatcher block from atmosphere could be confirmed by time domain reflectometry.

In cooldown tests the minimum reachable temperatures at different positions were measured. The results are shown in Table 1. It is remarkable, that compared to the cryogenic tests of the FoS cryocatcher in the universal cryostat at GSI [5] even lower temperatures were reached. Here the chamber reached 5.6 K andd the flanges even only 37.5 K and 61 K. The adjacent and actively cooled quadrupole chambers provide cooling power, why the flanges and bellows now also can be assumed to have temperatures below 18 K and such providing pumping speed for hydrogen.

## CRYOCATCHER IN SERIES QUADRUPOL MODULE

The distance of the cryocatcher block to the beam axis can be adjusted with stainless steel spacers from insulation vacuum side of the support structure. Different beam optics and resonant particles travelling with large amplitudes during the slow extraction process do not allow to set all cryocollimatos as close as possible to the the beam axis. Since the collimation efficiency decreases with increasing collimator distance to the beam axis, ion optical calculations are used to set individual cryocatcher distances for each position. During the intregration process into the quadrupole module, the required spacers are mounted. Figure 6 shows the different stainless steel spacers. In order to distinguish them easyliy without additional measurement tools, the different types have different characteristics, like beeing coloured or having a milled groove. Details are shown in Table 2.

Table 1: Temperature Achievements at the Cryocatcher During Cryogenic Tests in the FoS Quadrupole Module

| | |
|---|---|
| Copper shell, opposite to cooling profile | 4.6 K |
| Difference cooling profile - copper shell | 0.2 K |
| Flange US | 8.3 K |
| Flange DS | 10.8 K |

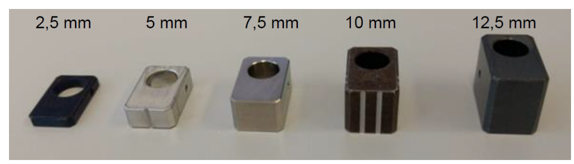


Figure 6: Different stainless steel spacer to adjust the cryocatcher's position with respect to the beam axis.

Table 2: Different Spacers with Their Characteristics and Yielding Distance of the Cryocatcher to the Beam Axis

| **Spacer** | **Characteristics** | **Cryocatcher Distance** |
|---|---|---|
| 2.5 mm | colored | 35 mm |
| 5 mm | silver with groove | 37.5 mm |
| 7.5 mm | silver | 40 mm |
| 10 mm | colored, two grooves | 42.5 mm |
| 12.5 mm | colored | 45 mm |

## SUMMARY AND OUTLOOK

The series procuction of 60 series cryocatcher has been finished after a total production time of three years including FoS, intensive tests and series optimization. The manufacturing process was accompanied by a detailed test procedure. Each test was either needed by regulations or necessary to assure the required and consistent quality.

The FoS cryocatcher was sucessfully integrated into the FoS quadrupole module and passed further tests. The achieved temperature distribution will provide high pumping speed to assure a reliable operation with heavy ion beam. The first series cryocatchers are now beeing integrated into the series quadrupole modules.

ISBN: 978-3-95450-214-1 ISSN: 2673-5490 doi:10.18429/JACoW-IPAC2021-WEPAB355



## REFERENCES

[1] L. H. J. Bozyk, D. H. H. Hoffmann, H. Kollmus, and P. J. Spiller, "Development of a Cryocatcher Prototype for SIS100", in *Proc. 1st Int. Particle Accelerator Conf. (IPAC'10)*, Kyoto, Japan, May 2010, paper THPEC078, pp. 4238–4240.

[2] L. H. J. Bozyk, D. H. H. Hoffmann, H. Kollmus, P. J. Spiller, and M. Wengenroth, "Construction and Test of a Cryocatcher Prototype for SIS100", in *Proc. 2nd Int. Particle Accelerator Conf. (IPAC'11)*, San Sebastian, Spain, Sep. 2011, paper TUPS007, pp. 1527–1529.

[3] L. H. J. Bozyk, H. Kollmus, and P. J. Spiller, "Development of a Cryocatcher-System for SIS100", in *Proc. 3rd Int. Particle Accelerator Conf. (IPAC'12)*, New Orleans, LA, USA, May 2012, paper THEPPB004, pp. 3237–3239.

[4] L. H. J. Bozyk, D. H. H. Hoffmann, H. Kollmus, and P. J. Spiller, "Development of a cryocatcher prototype and measurement of cold desorption", *Laser and Particle Beams*, vol. 34, no. 3, pp. 394–401, Apr. 2016. doi:10.1017/S0263034616000240

[5] L. H. J. Bozyk, S. Ahmed, and P. J. Spiller, "The First-of-Series SIS100 Cryocatcher", in *Proc. 9th Int. Particle Accelerator Conf. (IPAC'18)*, Vancouver, Canada, Apr.-May 2018, pp. 930–933. doi:10.18429/JACoW-IPAC2018-TUPAF084